Engineering Failure Analysis 135 (2022) 106137

Contents lists available at ScienceDirect

Engineering Failure Analysis

journal homepage: www.elsevier.com/locate/engfailanal

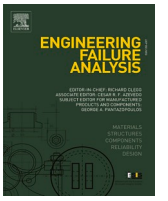

Failure investigation of a solar tracker due to wind-induced torsional galloping

David Valentín, Carme Valero *, Mònica Egusquiza, Alexandre Presas

Center for Industrial Diagnostics and Fluid Dynamics (CDIF), Polytechnic University of Catalonia (UPC), Av. Diagonal, 647, ETSEIB, 08028 Barcelona, Spain

ARTICLE INFO

Keywords:
Solar power
Galloping
Flutter
Solar tracker
Aeroelasticity

ABSTRACT

Solar power installations are increasing every year due to the decarbonization policy established around the world. Photovoltaic (PV) systems and specifically one-axis solar trackers are the most used type of installations in solar power plants. Those solar trackers are slender structures installed in open-air areas sometimes subjected to high speed winds. During the last years, failures in these structures are starting to appear, and most of them are related to a dynamic phenomenon called torsional galloping. The torsional galloping is an aeroelastic instability that presents very high deformation amplitudes and can be triggered at certain wind speeds and tilt angles of the solar tracker.

In this paper, a failure investigation of a solar tracker due to torsional galloping is carried out. The broken structure has been analyzed in the field and a numerical model of the structure has been built up. The numerical model is used to identify the natural frequencies of the structure as well as the maximum stresses in the different pieces of the solar tracker. The numerical investigation confirmed that the cause of the failure was torsional galloping occurring for high speed winds and with a tilt angle of the solar tracker of 0 degrees.

1. Introduction

During the last years the amount of solar power installed in the word have increased substantially. In 2019, about new 114 GW photovoltaic (PV) systems were installed in the world [1]. Most of the PV installations are based on large solar tracker arrays that follow the sun during the day changing their tilt angle to maximize their energy generation. There are trackers that only tilt from east to west and vice versa (one-axis tracker) and that can also tilt from north to south and vice versa (two-axis tracker). However, the most installed type is the one-axis tracker since they are simpler and cheaper structures. Those solar trackers are flat plates type structures installed in open-air areas where sometimes the wind can reach high speeds (see Fig. 1). Failures in solar trackers induced by high speed winds have started to appear recently.

The effect of the wind in flat plates have been studied in the past [2], experimentally [3,4] and numerically (in 2D [5,6] and in 3D [7,8]). In those studies, the static and dynamic effects of the wind for different velocities and tilt angles of the flat plate were studied in detail. The static forces that the wind induces on a solar array are decomposed into drag (parallel to the ground) and lift (perpendicular to the ground) forces, which create a torque about the support bar. For flat plates, the changes in the torque due to the tilt angle are known [9], with the minimum value at 0 degrees, and two inflection points: the first one around 5–7 degrees and the second one

* Corresponding author.
E-mail address: m.del.carmen.valero@upc.edu (C. Valero).

https://doi.org/10.1016/j.engfailanal.2022.106137
Received 21 October 2021; Received in revised form 17 January 2022; Accepted 7 February 2022
Available online 17 February 2022

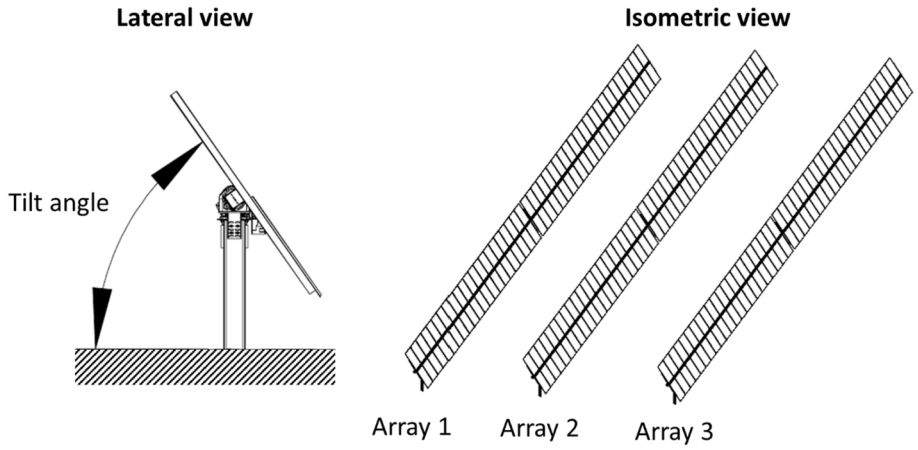

Fig. 1. One-axis solar tracker geometry.

around 40 degrees. However, the most challenging point in the structural design of solar trackers is to consider the dynamic effects of the wind. The most important dynamic wind mechanisms that can endanger the structural health of solar trackers are resonant vibration and the torsional flutter or galloping [10,11].

The resonant vibration mechanism occurs when the solar tracker is excited at its natural frequencies. It is caused either by wind buffeting or by the turbulence generated by other upwind trackers. It can be also caused by the lock-in phenomenon [12], where the vortex shedding frequencies coincide with one natural frequency of the structure. The vibration of the solar tracker can be high at those phenomena but they are not normally the cause of the largest failures, since the structure is rather flexible and deformable.

The torsional flutter or galloping are self-excited aerodynamic instabilities that are able to lead to very large amplitudes in torsional motion. Since both phenomena are of a very similar nature, the torsional flutter generally couples also vertical motion while the torsional galloping is an unidirectional twisting of the structure or an oscillatory motion depending on the torsional stiffness [11]. The oscillatory motion is given at the first torsional natural frequency of the solar tracker, which is usually at low frequency (below 3 Hz), since these structures are very large and slender. Those phenomena are very dangerous for the structural integrity since they are self-excited and once they occur, the amplitude of the motion increases progressively as the conditions change. For a given solar tracker, those phenomena can start for a certain wind velocity and tilt angle. Different failures due to flutter or galloping are explained in the literature but not specifically for solar trackers [13–16].

During the installation of a new solar plant in the south of Spain, one of the solar trackers was found catastrophically broken. At the moment of the failure the solar tracker was at a tilt of 0 degrees and the wind reached 60 km/h approximately. With this tilt angle, the static forces are almost negligible, therefore the cause of the damage had to be from a dynamic mechanism, such us the torsional galloping. In this paper, the damage found in this solar tracker is presented and analyzed. A numerical model has been used to confirm the origin of the damage, calculating the natural frequencies and stresses in the different parts of the structure when it is subjected to a large wind load.

2. Torsional galloping in solar trackers

The torsional movement of a solar tracker type of structure is defined by the following equation [17]:

$$I_0\ddot{\theta} + 2I_0\xi\omega_0\dot{\theta} + k\theta = M \tag{1}$$

where I_0 is the torsional inertia, ω_0 is the natural torsional frequency, ξ is the torsional damping, k the torsional stiffness, and θ is the angular displacement variable. M is the aerodynamic torque, which can be written as a function of the flutter derivatives for the study of the torsional galloping [18]:

$$M = \frac{1}{2}\rho U^2 b^3 (K\frac{b}{U}A_2^*\dot{\theta} + K^2 A_3^*\theta) \tag{2}$$

where K is the reduced frequency (inverse of reduced velocity), ρ is the air density, U the air velocity, b the characteristic length, and A_2* and A_3* are the flutter derivatives. These flutter derivatives are aerodynamic and function of the reduced velocity. Matching Eq. (1) and (2), the resulting differential equation will be unstable if the damping is negative [19]:

$$\xi - \frac{\rho U b^3 K A_2^*}{2I_o\omega_0} < 0 \tag{3}$$

With Eq. (3), the critical velocity for the torsional galloping can be obtained. For the solar tracker geometry, A_2* depends on the tilt angle, so the critical velocity too. Therefore, the instability occurs when A_2* changes the sign (goes from negative to positive) and this only occurs for a fixed value of reduced velocity (1/K). Therefore, the principal variables that are involved in the torsional galloping in

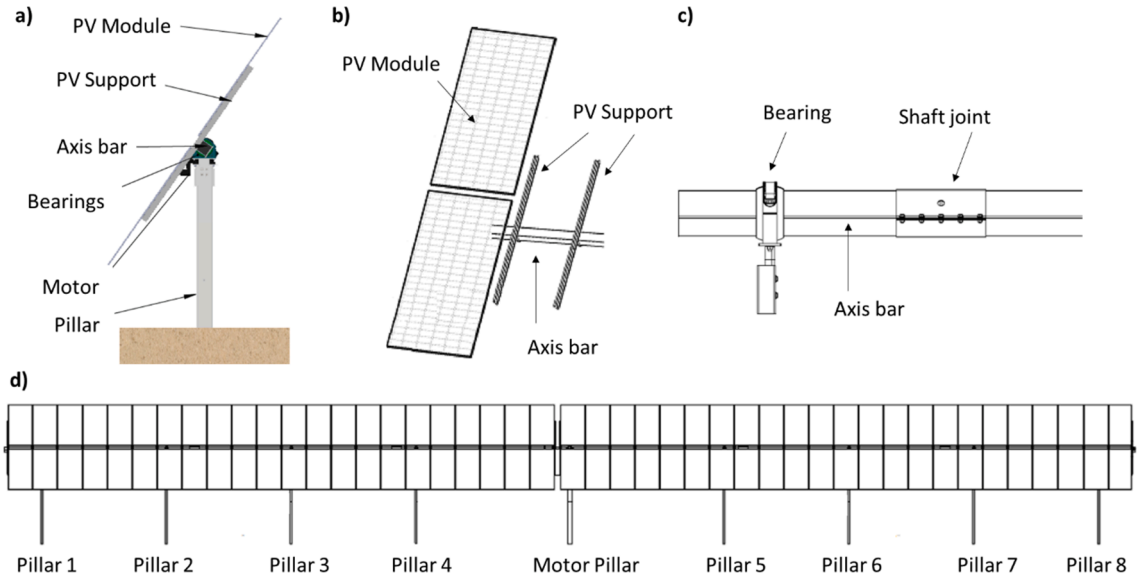

Fig. 2. Solar tracker geometry. a) Lateral view. b) Detail of the PV Modules and supports. c) Detail of bearings and shaft joint. d) Front view of the solar tracker.

Table 1
Materials of every component of the solar tracker.

Component	Material	Size	Weight
PV Module frame	Aluminum	2.016x998x25 mm	3.7 kg
PV Support	S350GD Steel	Omega Profile 30x80x27x1,8 mm	8.5 kg
Axis bars	S355JR Steel	Section: 150x150x3 mm	94.8 – 105.2 kg
Motor Pillar	S275JR Steel	HEB – 180, L = 3.523 *m*	50.2 kg
Pillars	S355JR Steel	C Profile, 230x80x30x3 mm, L = 3.6 *m*	24.8 kg
Bearings	Plastic Polyamide	Axis 150 mm	2.6 kg

solar trackers are the wind velocity, the tilt angle, the dimensional characteristics of the tracker and its torsional inertia and stiffness.

3. Damage description

3.1. Solar tracker description

The solar tracker analyzed in this study is part of a solar powerplant in Andalusia, in the south of Spain. It is a long structure of 45 m long formed by 90 PV modules that are subjected with an omega-type support to the axis bar (see Fig. 2). The axis is formed by 6 different square-section bars united by four different unions (see Fig. 2c) and fixed to the motor, which is the one in charge of rotating the PV modules depending on the sun position. The axis bars are supported by 8 different pillars with a bearing, that only restrain the bar in the vertical motion (perpendicular to the ground). The PV modules are formed by an aluminum frame with the PV material inside. Those modules are screwed to their supports by the aluminum frame (see Fig. 2b). The materials of every component of the solar tracker are shown in Table 1.

3.2. Damaged solar tracker

After a windy day, the solar tracker was found completely broken, as it can be observed in Fig. 3. It is seen that almost half of the tracker has rotated about 300 degrees from the initial position (0 degrees). Some PV modules are missing and others are broken. Furthermore, the supporting pillars 6, 7 and 8 (see Fig. 2) are completely bended. In Fig. 4 it is observed that the PV Modules near the pillar 5 and their supports are separated from the axis bar. In addition, it is seen that the axis bar that goes from motor pillar to pillar 5 is completely deformed in the junction with the other bar. This is the first sign that shows that the solar tracker was subjected to a high torsion force.

Looking with more detail into the area where the PV Modules are separed from the rest (Fig. 5), it is observed than the photovoltaic material is intact in the PV Modules found on the ground, but their frames are broken. This means that they were subjected to a high force that was able to bend the frame of those modules and separate them from the rest. In the same picture, one can see that the

Fig. 3. Damaged solar tracker.

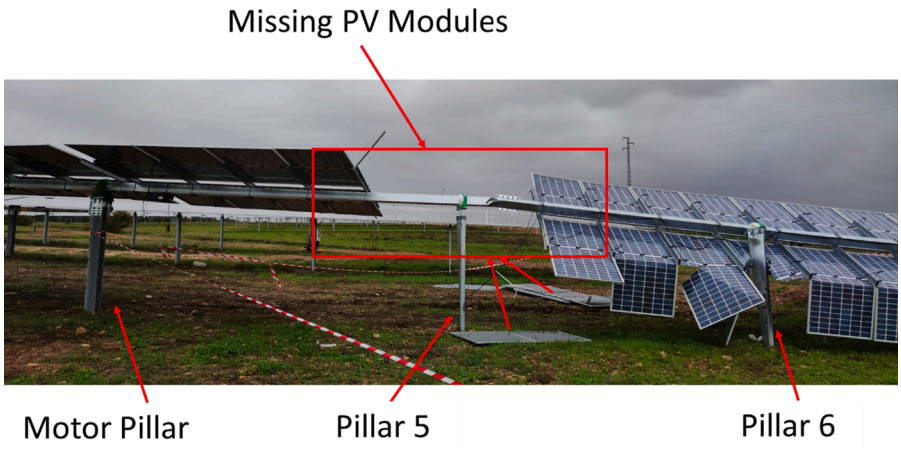

Fig. 4. Detail of the PV Modules near the pillar 5.

deformation in the axis bar is due to a high torsion producing plastic deformation. The way of how this bar is deformed discards any possibility of failure due to fatigue and points to a possible failure due to torsional galloping.

The rest of the PV modules that are still united to the axis bar are folded or broken because they hit the ground during the whole rotation of the axis. In Fig. 6 it is observed that only one row of PV Modules is bended at the junction between their supports and their frames. Furthermore, those modules that coincide with a pillar are totally destroyed due to the crash with them. The pillars present a large plastic deformation. This picture suggest that the whole solar tracker was deformed torsionally in clockwise direction (looking the axis bar from the tip shown in Fig. 6).

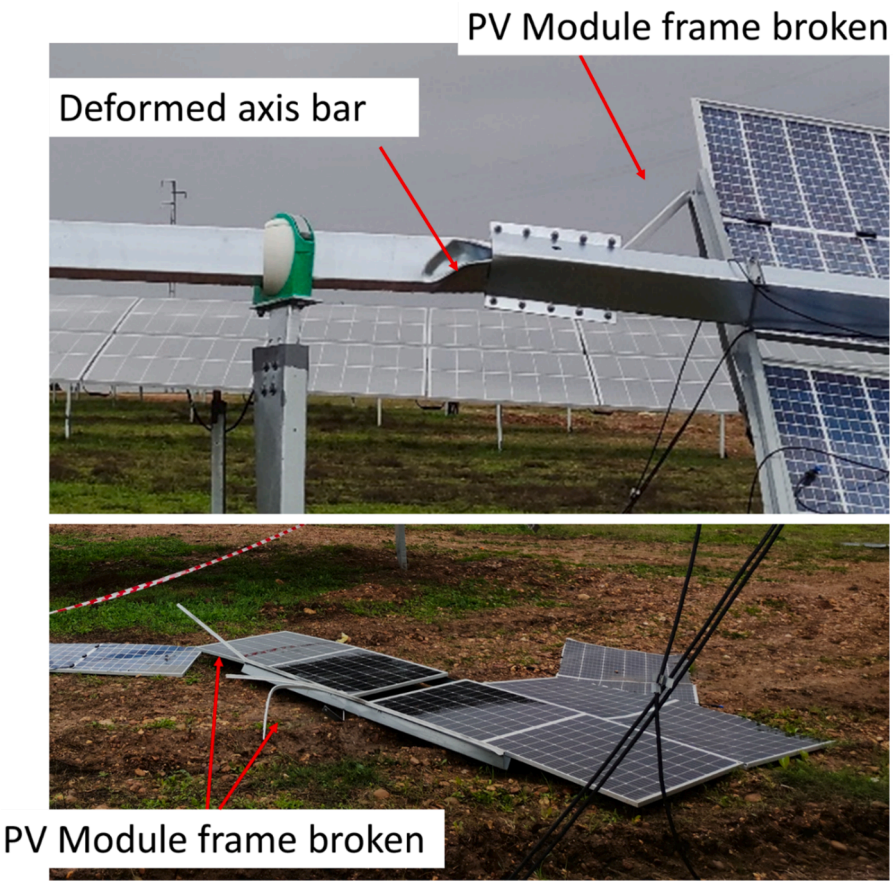

Fig. 5. Detail of the deformed axis bar and the broken PV Module frames.

Fig. 6. Detail of the bended and broken PV modules.

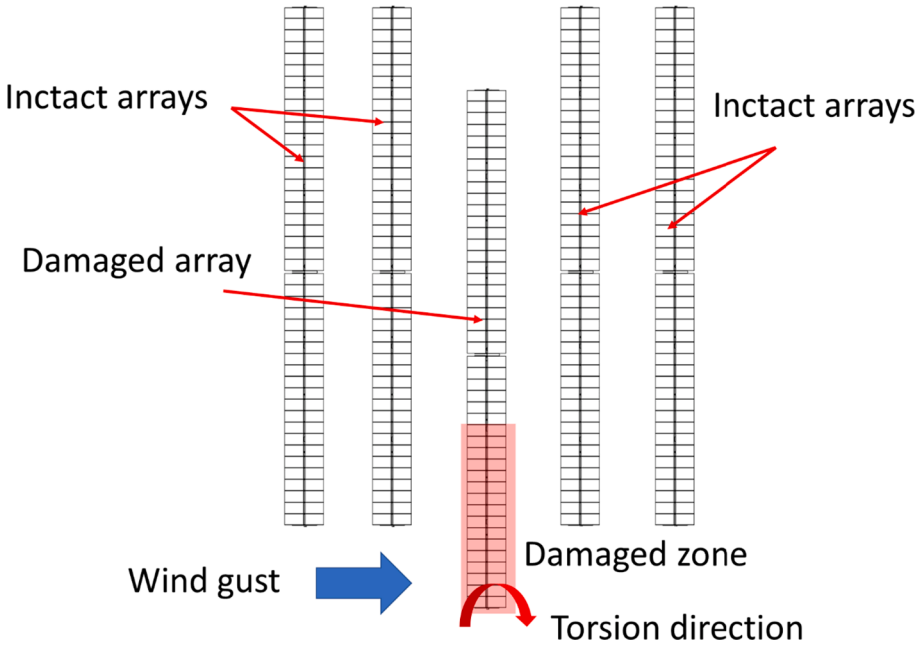

Fig. 7. Disposition of the damaged solar tracker in the solar plant.

3.3. Hypothetical causes of the damage

The damaged solar tracker has a special disposition in the solar plant (see Fig. 7). In the damaged part of the tracker there is not any other solar tracker upstream or downstream, which means that this part is directly subjected to the wind, without any obstacles before or after the tracker. This means that the torque due to the wind in this zone could be higher than in the rest of the tracker. Considering this fact and analyzing the damages presented in Fig. 3 to Fig. 6, the possible causes of the damage can be explained as follows:

1. The solar tracker was subjected to a wind gust of about 60 km/h according to data obtained in a nearby weather station.
2. The damaged part of the solar tracker was directly subjected to the wind gust since it has no obstacles before or after.
3. The solar tracker was fixed at 0 degrees tilt, where the static forces are minimum, therefore a dynamic phenomenon has to be the cause of such big deformations.
4. The deformation of the solar tracker is of torsional nature, which makes to think that the torsional galloping mechanism is the cause of this damage. This mechanism could have been triggered by the wind gust or the wind turbulence itself. Once this phenomenon is triggered, the amplitude of deformation is amplified until the structure breaks by plastic deformation.
5. Four PV Modules were found separated from the axis near pillar 5, which leads to think that they suffered the maximum torsional stress. In addition, their frames were found broken.
6. The axis bar junction near those modules was totally deformed, which means that the maximum torsional stress was located also in this zone.
7. Once those modules were separated from the axis bar due to the high torsional stress, the structure was divided into two parts which could further concentrate the torsional galloping effects on the damaged part.
8. The structure rotated 300 degrees, deforming pillars 6, 7 and 8 and colliding the PV modules of the right row with the ground. In the collision with the ground, those PV modules were deformed and the ones that coincide with a pillar were destroyed.

Therefore, the hypothetical sequence of events leading to the failure is the following:

1. Large wind gust acting over the solar tracker fixed at 0 degrees tilt.
2. The torsional galloping phenomenon is triggered and the structure starts to suffer large torsional deformation.
3. The PV Modules near pillar 5 suffer from large stress in their supports which broke and they got separated from the axis bar.
4. The torsional deformation continued increasing until the whole structure rotated about 300 degrees colliding with the ground and deforming the PV modules and the pillars 6, 7, 8.

To corroborate the hypothesis, a numerical model of the solar tracker has been built up and a numerical study including modal analysis and stress hot spots identification has been carried out.

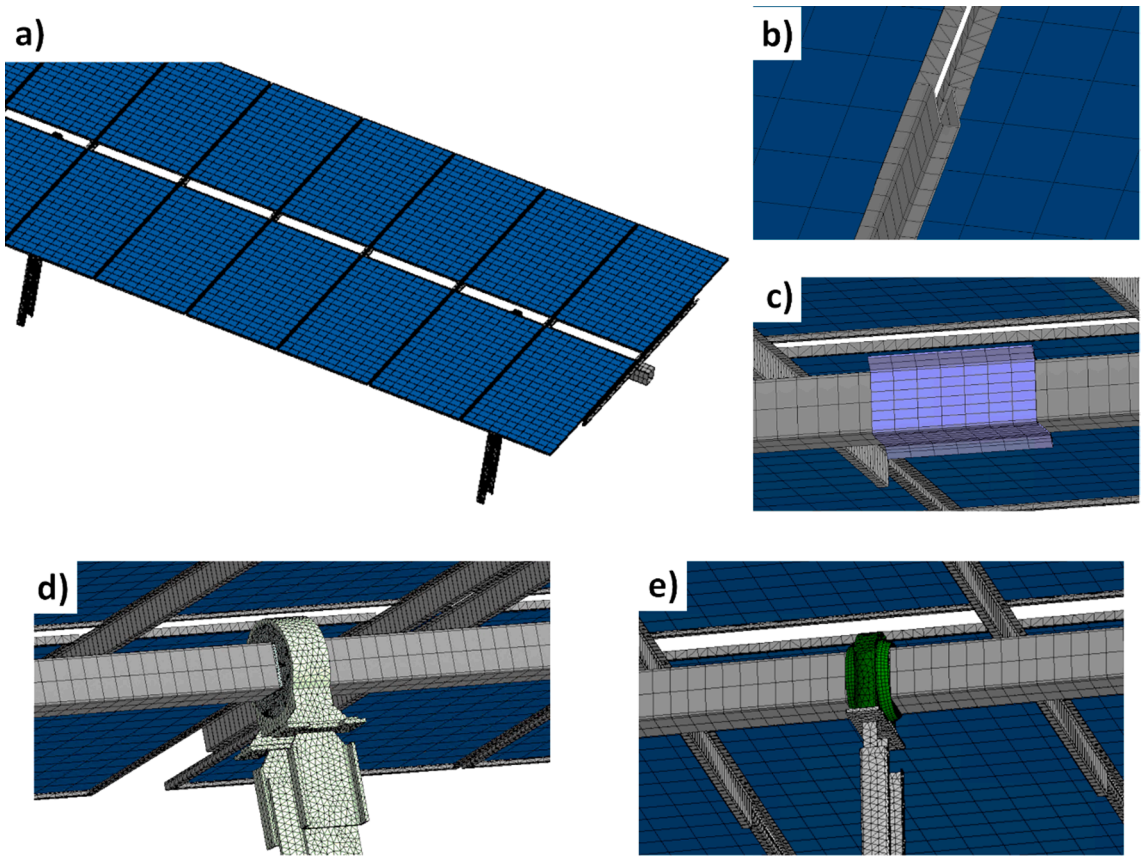

Fig. 8. Mesh detail. a) PV modules. b) Junction between the PV modules and their frame. c) Junction between axis bars. d) Motor pillar. e) Bearing detail.

4. Numerical study

4.1. FEM model

A FEM Model has been built up using the commercial software Ansys v2020 [20]. The geometry, mesh and boundary conditions used are explained in the next sections.

4.1.1. Geometry

The geometry was built from sketches. It consists of the whole solar array tracker, including the 9 pillars, the 6 axis bars, the bearings, the 90 PV modules including their frame and their union to the axis bar.

4.1.2. Mesh

Every part of the geometry was meshed separately and then joined by the use of contacts or junctions. Hexahedral elements were used for the PV modules and supporting bars and tetrahedral elements were used for the pillars, bearings and frames due to their more complex geometry. A mesh sensibility analysis was carried out with the results obtained for the modal analysis. The optimal mesh was obtained changing the element size since the results changed less than 1%. The optimal mesh had about 830.000 and $2.2{\cdot}10^6$ elements. The mesh is shown in Fig. 8.

4.1.3. Boundary conditions

The material properties for the simulation are the standard corresponding to the materials listed in Table 1. For the PV module the Young's Modulus, Poisson's ratio and density were set as $E = 2.1e9$ Pa, $\upsilon = 0.4$ and $\rho = 1370$ kg/m^3 respectively, according to reference data found in [21].

The pillars were fixed at their bottom with a non-displacement condition. Bonded contacts were defined between the PV modules and their supports bars and frames, and between the axis bars and their junction. The bearings were defined as a revolute joint, which permits only the angular displacement between the axis bar and the pillar. The motor pillar was fixed to the axis bars with a bonded contact, which is the normal situation when the solar tracker is fixed at certain tilt angle.

Table 2
Natural frequency values for the solar tracker.

Mode-shape number	Mode-shape name	Frequency [Hz]
1	B1	2.17
2	T1	2.19
3	T2	3.24
4	T3	3.30
5	T4	4.06

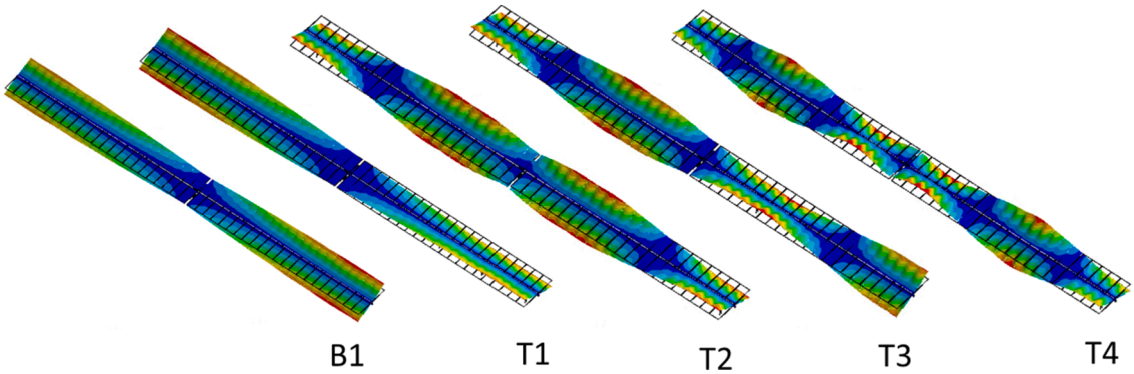

Fig. 9. Mode-shapes of the solar tracker. Normalized displacement (Red maximum, blue minimum).

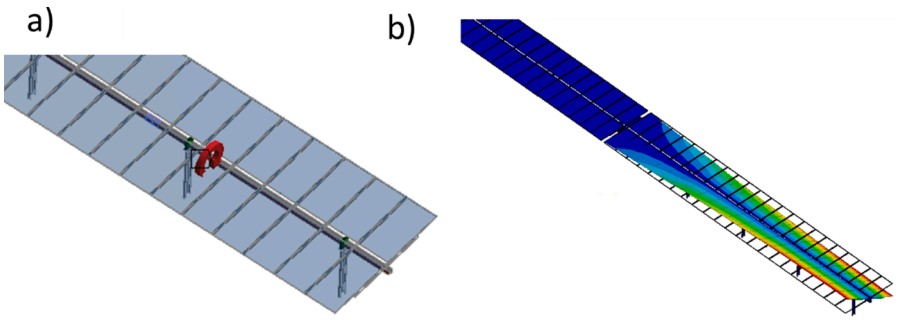

Fig. 10. a) Moment applied to the structure. b) Deformation of the structure due to the moment. Normalized displacement (Red maximum, blue minimum).

4.2. Modal analysis

First, a modal analysis was carried out to identify the natural frequencies and mode-shapes of the solar tracker. The natural frequencies found are summarized in Table 2 and their corresponding mode-shapes can be seen in Fig. 9. The mode-shapes have been classified as bending modes (B) and torsional modes (T). Only one bending mode is found at low frequency while several torsional modes are obtained in the range 0–5 Hz. The torsional modes appear with more nodal lines when increasing frequency. As explained in the introduction section, the first torsional mode (T1) is the one that is usually excited during the torsional galloping.

4.3. Stress analysis

A stress analysis was conducted to find the location of the maximum stresses in the structure when it is subjected to a high load due to the wind. A torque moment was applied on the axis of rotation of the structure as it is observed in Fig. 10. The amplitude of this torque was set to 10 kNm, according to [22] for a wind speed of 60 km/h.

Under these circumstances, the maximum stress was found at the shaft joint, and concretely in the nearest union of the pillar motor (see Fig. 11). This is the same union piece that was found completely deformed in the field (Fig. 5). Looking at the stress, piece by piece of the structure, one can find the maximum stresses in those parts were each piece was broken. Fig. 12a shows the stress in the PV supports and the maximum is located in the union with the axis bar near Pillar 5, fact that explains why the PV Modules were found separated from the axis bar in the field. The PV Module frames present also the maximum stress (see Fig. 12b and c) in that zone where they were completely bended (Fig. 6).

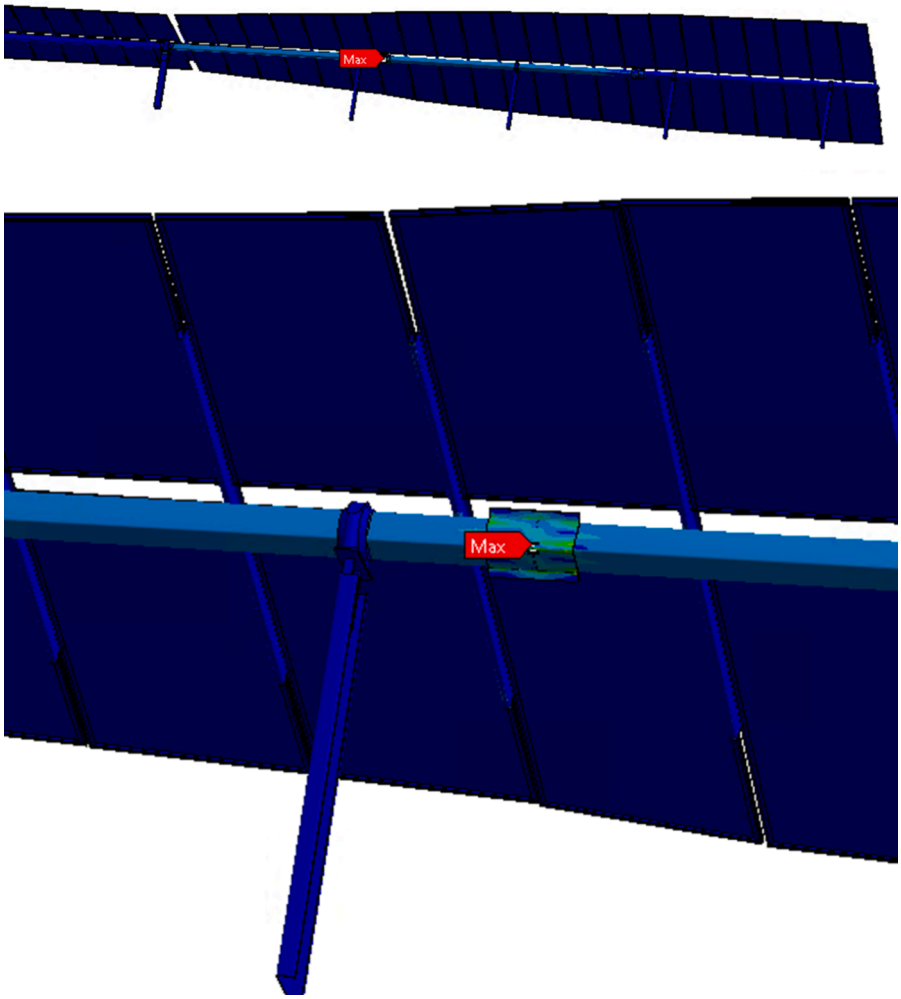

Fig. 11. Maximum stress in the solar tracker. Normalized stress (Red maximum, blue minimum).

Therefore, the numerical simulation confirms the initial hypothesis presented in section 3.3, determining that the weakest pieces under a torsional galloping phenomenon are shaft joints, the PV supports and the PV Module frames. Moreover, the disposition of the solar trackers in the plant (Fig. 7) makes the wind force to be higher at the damaged zone, leading to a torque moment like the one applied in the simulation. Furthermore, the torsional deformation of the panel and the maximum stresses found in the simulation coincides with the shape of the first torsional mode-shape (T1), demonstrating that the torsional galloping phenomena occurred.

5. Possible actions to avoid future failures

In order to avoid failures due to torsional galloping in solar trackers, different actions or measures can be taken. As one can see in section 2, the torsional galloping depends on the structural properties and dimensions of solar trackers, the tilt angle and the wind characteristics. As the wind is not controllable at all, the actions to avoid this phenomenon should be taken by acting over the structure properties or the tilt angle. The structure dimension is defined by the amount of power generated, so it is generally fixed for every power plant. Therefore, the best possibility acting over the structure would be to increase its torsional stiffness. To do that, different options are possible, from changing the material and profile of the axis bar, to add extra supports to the PV Modules. However, these measures add extra costs to the installation.

Another option is to act on the tilt angle. It is known that the phenomenon is more prone to occur when the solar tracker is near 0 degrees and that at larger tilt angles such us 45 degrees, it is less likely to occur [19]. Therefore, when large wind speed is detected, the tilt angle should be changed to a safer position. This will reduce the amount of solar power generated at that moment but it will decrease the probability of triggering the torsional galloping phenomenon. To do that, an efficient monitoring system in real time should be used, which has to be able of monitoring the wind parameters at the same time than the solar tracker vibration or torsional deformation. A solution to detect and avoid torsional galloping in solar tracker was presented in [23] by this group of authors.

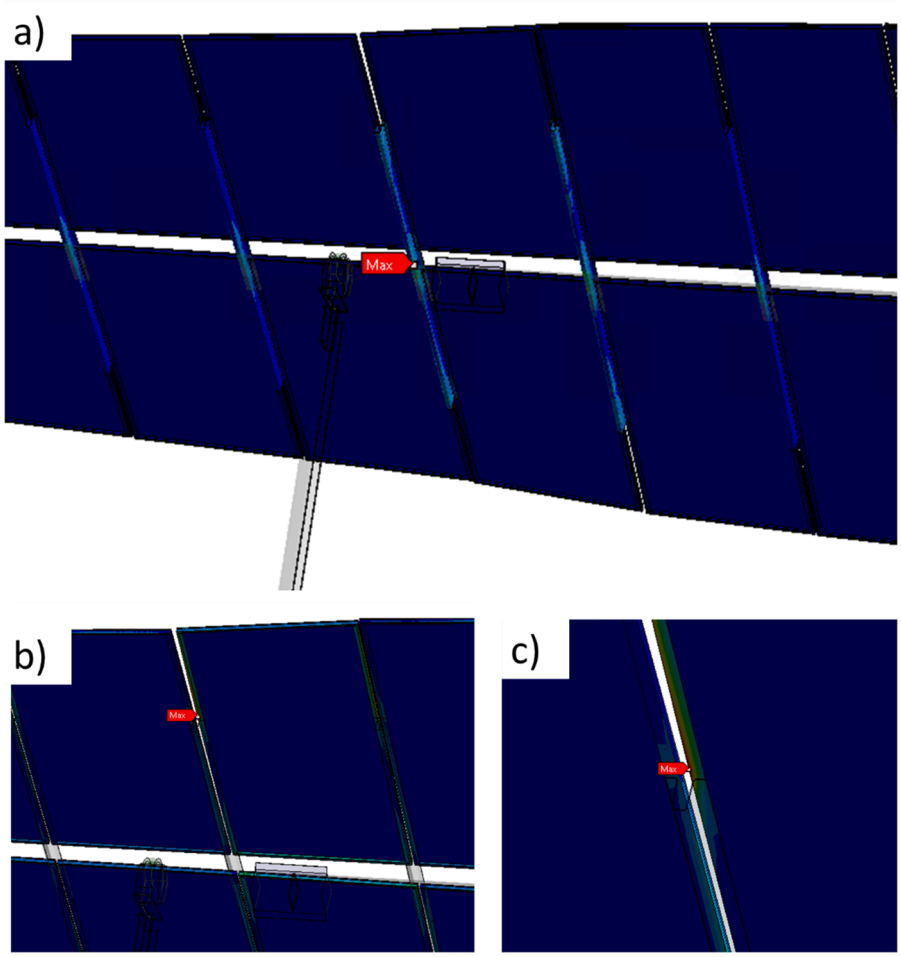

Fig. 12. a) Stress in the PV supports. b) Stress in the PV module frames. c) Detail of the stress in the PV module frame. Normalized stress (Red maximum, blue minimum).

6. Conclusions

A failure investigation of a solar tracker was carried out in the present paper. After a windy day, one of the solar trackers of the power plant was found catastrophically broken. The pictures in the field show that the structure was deformed drastically due to a high torque in the axis. The high plastic deformation in some parts of the structure lead to the PV modules to contact the ground and to break after that. The solar tracker was fixed at 0 degrees tilt angle at the moment of the accident, where the static wind forces are minimum. Therefore, the phenomenon leading to that high torsional motion vibration amplitudes ought to be the torsional galloping according to previous experiences in solar trackers.

To confirm the cause of the damage, a numerical model was built up. A modal analysis was carried out to find the main natural frequencies of the structure. The first torsional mode shape was identified, which is the one excited during the torsional galloping. Furthermore, a stress analysis was performed with the same numerical model. A torque was applied in the axis bar and the location of the maximum stresses were identified. These locations coincide with those pieces that were found deformed or broken in the field, which confirms that the torsional galloping was the cause of the catastrophic failure.

Declaration of Competing Interest

The authors declare that they have no known competing financial interests or personal relationships that could have appeared to influence the work reported in this paper.

Acknowledgements

Authors would like to acknowledge Endesa for making accessible the solar tracker as well as its geometry. David Valentín and

Alexandre Presas acknowledge the Serra Húnter program.

References

[1] International Energy Agency, IEA PV Snapshot 2019, 2020. https://iea-pvps.org/wp-content/uploads/2020/04/IEA_PVPS_Snapshot_2020.pdf.
[2] M. Shademan, A. Naghib-Lahouti, Effects of aspect ratio and inclination angle on aerodynamic loads of a flat plate, Adv. Aerodyn. 2 (2020) 1–23.
[3] A. Fage, F.C. Johansen, On the flow of air behind an inclined flat plate of infinite span, Proc. R. Soc. London. Ser. A, Contain. Pap. a Math. Phys. Character. 116 (1927) 170–197.
[4] G.B. Schubauer, H.L. Dryden, The effect of turbulence on the drag of flat plates, US Government Printing, Office (1935).
[5] K. Kuwahara, Numerical study of flow past an inclined flat plate by an inviscid model, J. Phys. Soc. Japan. 35 (5) (1973) 1545–1551.
[6] J.D. Hudson, S.C.R. Dennis, The flow of a viscous incompressible fluid past a normal flat plate at low and intermediate Reynolds numbers: the wake, J. Fluid Mech. 160 (1985) 369–383.
[7] KUNIHIKO Taira, TIM Colonius, Three-dimensional flows around low-aspect-ratio flat-plate wings at low Reynolds numbers, J. Fluid Mech. 623 (2009) 187–207.
[8] A. Hemmati, D.H. Wood, R.J. Martinuzzi, Characteristics of distinct flow regimes in the wake of an infinite span normal thin flat plate, Int. J. Heat Fluid Flow. 62 (2016) 423–436.
[9] L. Pigolotti, C. Mannini, G. Bartoli, Experimental study on the flutter-induced motion of two-degree-of-freedom plates, J. Fluids Struct. 75 (2017) 77–98.
[10] E. Young, X. He, R. King, D. Corbus, A fluid-structure interaction solver for investigating torsional galloping in solar-tracking photovoltaic panel arrays, J. Renew. Sustain. Energy. 12 (2020) 63503.
[11] M.A. Matthew T. L. Browne, M.Eng., P.Eng., Soltec Dy-Wind, (n.d.). https://soltec.com/dywind/ (accessed February 4, 2021).
[12] K.C.S. Kwok, W.H. Melbourne, Wind-induced lock-in excitation of tall structures, J. Struct. Div. 107 (1) (1981) 57–72.
[13] C. Klinger, Failures of cranes due to wind induced vibrations, Eng. Fail. Anal. 43 (2014) 198–220. https://doi.org/10.1016/j.engfailanal.2013.12.007.
[14] J.-S. Chou, C.-K. Chiu, I.-K. Huang, K.-N. Chi, Failure analysis of wind turbine blade under critical wind loads, Eng. Fail. Anal. 27 (2013) 99–118. https://doi.org/10.1016/j.engfailanal.2012.08.002.
[15] A. Rama Rao, B.K. Dutta, Blade vibration triggered by low load and high back pressure, Eng. Fail. Anal. 46 (2014) 40–48. https://doi.org/10.1016/j.engfailanal.2014.07.023.
[16] G. Fang, W. Pang, L. Zhao, K. Xu, S. Cao, Y. Ge, Tropical-cyclone-wind-induced flutter failure analysis of long-span bridges, Eng. Fail. Anal. 132 (2022), 105933. https://doi.org/10.1016/j.engfailanal.2021.105933.
[17] C. Rohr, P.A. Bourke, D. Banks, Torsional instability of single-axis solar tracking systems, in: Proc. 14th Int. Conf. Wind Eng. Porto Alegre, 2015: pp. 21–26.
[18] R.H. Scanlan, J.J. Tomko, Airfoil and bridge deck flutter derivatives, J. Eng. Mech. Div. 97 (6) (1971) 1717–1737.
[19] E. Martínez-García, E. Blanco-Marigorta, J. Parrondo Gayo, A. Navarro-Manso, Influence of inertia and aspect ratio on the torsional galloping of single-axis solar trackers, Eng. Struct. 243 (2021) 112682. https://doi.org/10.1016/j.engstruct.2021.112682.
[20] ANSYS(R), Ansys User's Manual 2020, (2020). https://www.ansys.com/.
[21] A. Kilikevičius, A. Čereška, K. Kilikevičien\.e, Analysis of external dynamic loads influence to photovoltaic module structural performance, Eng. Fail. Anal. 66 (2016) 445–454.
[22] Soltec; Dy-Wind, Dynamic Wind Analysis in Tracker Array Design, n.d.
[23] D. Valentín, C. Valero, M. Egusquiza, A. Presas, E. Egusquiza, Torsional galloping detection in solar trackers, in: Online Symp. Aeroelasticity, Fluid-Structure Interact. Vib. 14–15 Oct. 2021, 2021. https://www.aeroelasticity2021.com/.